Investigation of ethylene oxide-co-propylene oxide for dissolution enhancement of hot-melt extruded solid dispersions

Dean Hurley[1], Catherine B. Potter[2], Gavin M. Walker[2], Clement L. Higginbotham[1*]

[1]Materials Research Institute, Athlone Institute of Technology, Westmeath, Ireland

[2]Synthesis and Solid State Pharmaceutical Centre (SSPC), Bernal Institute, University of Limerick, Limerick, Ireland.

Correspondence to: Clement L. Higginbotham

Tel: +353-(0)-90-6468050

E-mail: chigginbotham@ait.ie

Abstract

The optimal design of amorphous solid dispersion (ASD) formulations requires the use of excipients to maintain supersaturation and improve physical stability in order to ensure shelf-life stability and better absorption during intestinal transit, respectively. Blends of excipients (surfactants and polymers) are often used within pharmaceutical products to improve the oral delivery of BCS class II drugs. Therefore in this study, a dissolution enhancer, poloxamer 407 (P407), was investigated to determine its effect on the dissolution properties and on the amorphous nature of the API contained in the formulation. Phase solubility studies of indomethacin (INM) in aqueous solutions of P407 and PVP VA64 showed an increase in the kinetic solubility of INM compared with the pure drug at 37°C with a K_a value of 0.041 µg/ml. **The solid dispersions showed a higher dissolution rate when compared to pure and amorphous drug when performed in pH buffer 1.2 with a kinetic solubility of 21 µg/ml**. The stability data showed that the amorphous drug in solid solutions with PVP VA64 and P407 remained amorphous and the % P407 loading had no effect on the amorphous stability of INM. This study concluded that the amorphous solid dispersion contributed to the increased solubility of INM.

Keywords: polymers, extrusion, glass transition, solid dispersion, amorphous, solubility, crystallization, materials science, physical characterization

1. Introduction

A growing number of drugs are being classified under the biopharmaceutical classification system (BCS) as poorly soluble. While this classification describes 40% of currently marketed drugs, the number rises to 90% for drugs in developmental pipelines.[1]

A commonly accepted approach in the formulation of BCS class II drugs, namely those which exhibit solubility difficulties only and have high permeability, is their incorporation into an amorphous solid dispersion with either one, [2–4] or two, [5,6] amorphous polymers. The role of polymer in the formulation is two-fold; to stabilize the amorphous active pharmaceutical ingredient (API) against recrystallization during storage,[7] and to prevent precipitation of the API from the supersaturated state during dissolution in the gastrointestinal tract.[8]

A number of comparative studies of identical formulations of API and polymer(s) produced using different processing techniques have shown differences in the amorphous stability during storage and the dissolution behavior of amorphous solid dispersions. **There are multiple factors that can potentially affect the dissolution rate and extent of dissolution of ASDs, such as glass transition temperature, preparation method (examples include supercritical fluid technology, fusion/solvent evaporation method and freeze drying etc.), preparation conditions (for example, cooling rate, freezing, processing time and temperature). Humidity, mechanical stress and temperature can also affect the dissolution rate of ASDs.[9]**

Semi-crystalline polymers such as polyethylene oxide and its derivatives, are often used as aqueous dissolution enhancers or surfactants and have also been used as plasticisers for hot melt extrusion. Poloxamer 188, a block copolymer of poly(propylene oxide) and poly(ethylene oxide) was used as a plasticiser for the poorly soluble API - amorphous polymer system, Aripiprazole – Poly (vinylpyrrolidone) K30 to allow processing by hot melt extrusion despite the relatively high glass transition temperature (T_g) of Poly (vinylpyrrolidone) K30.[10] The same study also commented on enhancement of the initial rate of dissolution exhibited by the addition of only 5% w/w of the plasticizer.

The addition of a surfactant in the solid dispersion itself could help maintain the degree of supersaturation achieved by the amorphous drug during the dissolution of the solid dispersion [11]. However, the addition of a low Tg, polymeric excipient such as poloxamers to an amorphous dispersion could contribute to solid state instability of the amorphous drug either by increasing the mobility of the dispersion through lowering the glass transition of the mixture or by acting as a nucleation site.[12,13]

Recently the mechanism of crystallisation of amorphous APIs in a number of semi-crystalline polymer matrices have been investigated and indicates a well-ordered crystallisation in accordance with the lamellar structure of Poly (ethylene glycol) PEG.[14] Furthermore Zhu *et al*. (2010) reported a number of model APIs which when melt quenched with Poly (ethylene glycol), molecular weight 3350 and transformed into the amorphous form, did not recrystallise immediately and which exhibited a degree of miscibility with the amorphous portion of the semi-crystalline polymer.[15] Similarly, Gumaste *et al*.[16] reported miscibility of itraconazole, poloxamer, and hydroxypropylmethylcellulose acetate succinate in the ratio 23:23:54 following exposure to 40°C/75% RH for 1 month after which time the itraconazole remained in the amorphous form.

Recent literature has focused on the use of binary mixtures to improve the dissolution properties of indomethacin (INM), however very little has been reported in literature on the use of ternary mixtures and the use of Poloxamer 407 (Ethylene oxide and propylene glycol copolymer) (P407) as a semi crystalline surfactant to enhance the aqueous solubility of INM using Poly (vinylpyrrolidone-vinyl acetate copolymer) (PVP VA64) as a polymeric carrier. Also, no literature has been published on the glass transition of poloxamer based polymers and its effect on the amorphous stability of solid dispersions.

2. Materials and methods

2.1. Materials

Crystalline γ-indomethacin (1-(4-Chlorobenzoyl)-5-methoxy-2-methyl-3-indoleacetic acid) (INM), purchased from Tokyo Chemical Industry (TCI) (Oxford Science Park, UK) (N.V.) (M_w 357.79 g/mol^{-1}, T_m 160.0 °C T_g 42°C) was used as a model drug. INM has an aqueous solubility of 1.5 µg/ml at pH 1.2.[17]

Poloxamer 407 (P407), a hydrophilic non-ionic surfactant, (Ethylene oxide and propylene glycol copolymer), (Mw 12,000, T_m 55°C, T_g -67°C) and Poly (vinylpyrrolidone-vinyl acetate copolymer) (PVP VA64) (Mw 45,000, T_g 107°C, T_m 140°C) was purchased from BASF Europe GmbH (Burgbernheim, Germany). All other reagents and chemicals were purchased from Sigma Aldrich (Wicklow, Ireland) and were of analytical reagent grade.

2.2. Preparation of physical mixtures

25 different combinations of the three components were studied and 10 g total powder was used for each sample. Powders were weighed and mixed thoroughly in a mortar and pestle for five minutes according to the compositions detailed in Table 1. Amorphous INM (aINM) was prepared by heating to 160°C in a stainless steel beaker using a hotplate and quench cooling using liquid nitrogen.

2.3. Hot melt extrusion

Hot melt extrusion was performed using a co-rotating Prism **16mm** Twin-screw extruder (Thermo Fisher Scientific, USA) with a 2mm diameter die and a length to diameter (L/D) ratio of **25/1**. Screws contained all-conveying elements and a screw speed of 60 RPM was used. The extruder was split into five heating zones which, from feeding zone to the die, had set points of 100, 120, 140, 160 and 160 °C. On exiting the die the extrudate was allowed to cool to 25°C then ground under liquid nitrogen in a mortar and pestle, and passed through a 200 µm sieve to obtain an appropriately sized fraction for further studies.

2.4. Calculation of Hansen solubility parameters (δ)

Preformation of drug and polymers was conducted using the Hansen solubility parameters which can be calculated using the combined group contribution methods of Van Krevelen-Hoftyzer and Fedors (Fedors. (1974)) and (Van Krevelan and Hoftyzer. (1976)),[9] by considering their chemical structural orientations and the molecular weights of each of the components. These are expressed by the following equation (Eq) 1:

$$\delta^2 = \delta^2_d + \delta^2_p + \delta^2_h \qquad \text{Eq. (1).}$$

Where,

$$\delta_d = \frac{\Sigma F_{di}}{V}, \ \delta_p = \frac{(\Sigma F_{pi}{}^2)}{V}{}^{1/2}, \ \delta_h = \left(\frac{\Sigma F_{hi}}{V}\right)^{1/2}$$

where *i* is the functional group within the molecule, δ is the total solubility parameter, δ_d is the contribution from dispersion forces, δ_p is the contribution of polar interactions, δ_h is the contribution of hydrogen bonding, F_di is the molar attraction constant due to molar dispersion forces, F_pi is the molar attraction constant due to molar polarization forces, E_hi is the hydrogen bonding energy and V is the molar volume.[18]

2.5. ATR-FTIR Spectroscopy

ATR-FTIR spectra were collected using a Perkin Elmer, Spectrum One fitted with a universal ATR sampling accessory. Data was collected in the spectral range of 4000-420cm^{-1}, utilizing a 16 scan per sample cycle and a fixed universal compression force of 80N. Subsequent analysis was carried out using Spectrum software.

2.6. X-ray powder diffraction (XRPD)

X-ray diffraction spectra were collected using a Philips PANalytical X'Pert MPD Pro with PW3064 sample spinner. The dried granules were gently ground using a pestle and mortar and placed on zero-background silica disks. The diffraction pattern was collected between 5 and 40° (2θ) with a step size of 0.0167°, a counting time of 29.845 s, and a sample rotation of 15 rpm using PANalytical Data Collector, version 2.0. The source was Cu Kα (λ = 1.5418 Å), the accelerating voltage was 40 kV, and the anode current was 35 mA. A fixed divergence slit of ¼" and a 0.020 mm nickel filter were used.

2.7. Differential scanning calorimetry (DSC)

DSC studies were conducted on a PerkinElmer DSC 8500 equipped with a refrigerated cooling accessory (PerkinElmer, UK). Helium, 30 mL/min, was used as purge gas. The instrument was calibrated using a heating rate of 100°C/min using high purity indium to standardize the temperature and heat flow signal. Then 1.0−2.5 mg samples were weighed and placed in crimped DSC pans. Samples were ramped from -10 to 180 °C at 100 °C/min.

The analysis was carried out using PerkinElmer Pyris Thermal Analysis software, version 10.1 and any numerical values reported are the average ± SD of three independently prepared samples. Samples from the accelerated stability studies were dried over phosphorous pentoxide for at least 24 h prior to analysis by hyper DSC to remove the significant moisture endotherm exhibited in non-dried samples.

2.8. Scanning Electron Microscopy (SEM)

Scanning electron microscopy (SEM) was performed on a Mira SEM (Rescan, Czech Republic) with a magnification of 100kx. Sample preparation involved placing samples on the sticky surface of aluminum stub using double sided sticky tape to increase the electrical conductivity of the sample. After sufficient time (10mins), the SD samples were coated with a thin layer of gold by placing the samples within a sputter coater (BAL-TEC SCD, sputter, USA) for 110sec at 0.1mBar vacuum. The SEM images were obtained using an acceleration voltage of 15 KV.

2.9. Phase solubility Studies

Solubility studies were performed in triplicate using the method reported by Higuchi and Connors (Higuchi et al., 1965) in pH buffer 1.2. An excess amount of INM was added to aqueous solutions of each carrier to increasing concentrations of both polymeric carriers in 10 ml volumetric flasks. The suspensions were maintained at 37 °C for 24 h. This duration was previously tested to be sufficient to reach equilibrium.

2ml aliquots were withdrawn and were filtered through 25mm Millex - LCR PTFE hydrophilic syringe filters (0.45 µm, Merck Millipore LTD, Ireland). The filtrates were suitably diluted if required and analyzed, spectrophotometrically for the dissolved drug at 320 nm. Shaking was continued until three consecutive readings were performed. The apparent 1:1 stability constant Ka was calculated from the phase solubility graph using the following equation:

$$K_a = \frac{\text{Slope}}{\text{So (1-slope)}} \qquad \text{Eq. (2).}$$

Where So is the intrinsic aqueous solubility of INM. The Gibbs free energy of transfer (ΔG^0_{tr}) of INM from pure water to the aqueous solution of carrier was calculated by the equation below.

$$\Delta G^0_{tr} = -2.303\ RT\ log\ So/Ss \qquad \text{Eq. (3).}$$

where S0/SS is the ratio of molar solubility of INM in aqueous solutions of carrier to that of the same medium without carrier.

2.10. *In-Vitro* Dissolution Studies

The release rate of INM from SDs and physical mixtures was determined under non-sink conditions using United States Pharmacopeia (USP) dissolution testing apparatus 1 (basket method) (Distek 50947, USA) with a paddle speed of 50 rpm. The dissolution test was performed using 900 ml of pH buffer 1.2 at a temperature of 37 ± 0.5°C.

A formulation equivalent to 100 mg of INM in SDs and physical mixtures were placed in dissolution medium, with 5 ml aliquots withdrawn at predetermined time intervals (0, 10, 17, 24,45 minutes and 1, 2 and 3 hours), and filtered through a 25mm Millex - LCR PTFE hydrophilic syringe filter (0.45 µm, Merck Millipore LTD, Ireland). At each time point, the same volume of fresh medium was replaced as withdrawn. The concentration of INM in each sample was determined using a UV-1280 UV-Vis spectrophotometer (Shimadzu, Japan) and a standard calibration curve.

Fresh dissolution medium was used as a blank. Pure INM was used as a control. The concentration of INM dissolved for each formulation (n =3) was plotted as a function of dissolution time with data being expressed as the average ± standard deviation of replicate absorbance measurements.

2.11. Statistical Analysis

The drug dissolution profiles of all SD formulations were compared using an analysis of variance (ANOVA) statistical test. The impact of the amorphous form on the area under the curve (AUC) was statistically examined using (ANOVA) (GraphPad Prism version 5.03 for Windows, GraphPad Software, San Diego, CA). Post-hoc comparisons of the means were performed using Tukey's Multiple Comparison test. A significance level of * $p < 0.05$ was accepted to denote significance in all cases.

2.12. Accelerated amorphous stability studies

Stability studies were conducted under accelerated conditions (40°C, 75% relative humidity) for 5 months by placing SDs in open class vials which were stored in a desiccator which contained a saturated solution of sodium chloride to generate a relative humidity of 75% RH. The relative humidity inside the desiccator was checked regularly using a thermohygrometer. The stored SDs were tested using DSC as previously described.

3. Results and discussion

3.1. Preformulation Studies

The Hansen solubility parameters (δ) were used to estimate the miscibility of the API INM and each of the polymers. Calculated Hansen solubility parameters specify the probability of a large molecular weight polymer to be miscible with a drug molecule. In the calculation, three specific forces were taken into account.

It is shown that the compounds that have similar values are more likely to be miscible as a result of balancing the energy of mixing that is released by various inter-molecular interactions between each of the components and the energy released by intra-molecular interactions between each of the components within the compounds. The Hansen solubility parameters were calculated by group contributions of dispersion forces, polar forces and hydrogen bonding forces using the Van Krevelen/Hoftyzer method.

Greenhalgh *et al.*[19] classify compounds based upon the differences in solubility parameters. If ***Δ***δ is less than 7 $MPa^{1/2}$ all the components are miscible and phase separation is less likely to occur. When ***Δ***δ value is greater than 7 $MPa^{1/2}$, both components are immiscible and phase separation can occur between drug and polymer.[20] **The solubility parameters (δ) of INM and commonly used HME polymers (Δδ) are shown in Table 2. As shown in Table 2, a difference in solubility parameter of (Δδ) $\leq$ 7.0 $MPa^{1/2}$ was observed between INM and P407 and PVP VA64; hence based on the solubility parameter theory, these polymers were further evaluated using ATR-FTIR spectroscopy, XRPD, DSC, SEM and *in-vitro* dissolution studies to examine drug-polymer miscibility.**

3.2. DSC and XRPD studies of extruded solid dispersions

Figures 1(a) and Figure 2(b) illustrates the DSC thermograms of each of the components as received and after a DSC cycle of heating to 180 °C and cooling. A glass transition was detected for P407 at -67 °C which is the expected value, between the known glass transitions for each of the homopolymers of this copolymer. This value has never been reported in the literature, a very low temperature was used for P407 to show the extremely low T_g as shown in **Figure 1(b).** The cooling rate used was 100°C/min, it could be commented that this cooling rate would stop the drug from recrystallizing, however, a slow cooling rate was tried as well and the drug still didn't recrystallize upon cooling. This may have been a result of the power compensated DSC.

The 725 g/mol molecular weight grade of poly(propylene oxide) has a T_g of around -85 °C [21], while the 1000 g/mol molecular weight grade of poly (ethylene oxide) exhibits a glass transition around -71.6 °C [22]. The value of the glass transition nor the enthalpy of the P407 melt changed significantly following heating and cooling. The DSC thermograms of pure INM, P407, PVP VA64 and SD formulations were recorded **(Fig. 1(a), Fig. 1(b) and Fig. 2(b)).** Pure INM showed a sharp endothermic peak at 158.16°C (T_m) and a T_g of 42.285°C. Pure P407 showed an endothermic peak at 58°C as it is semi-crystalline in nature. PVP VA64 was confirmed as amorphous as a single T_g at 109.94°C was observed and contained no sharp melt endothermic peak.

XRPD analysis (Fig. 2(a)) of the SD formulations confirmed the amorphous nature of INM within all SD formulations due to the slight halo raised above the baseline, due to the lack of any sharp, well-defined peaks in the diffractogram. P407 retained its semi-crystalline state in all SD formulations compared to the SD formulations prepared by Gumaste, Gupta and Serajuddin. [16] who reported that poloxamer was amorphous. However careful analysis of the SD formulations (Fig. 2(b)) indicates that the glass transition of P407 at -67°C was not present.

The effect of polymer and drug loading on the glass transition behavior of the ASD formulations was predicted using the thermodynamic models of Couchman and Karasz.[23,24] and the Simha-Boyer rule[25]. Using the simplified Couchman–Karasz equation for drug-polymer mixtures, the theoretical glass transition of the solid dispersions can be calculated as follows;

$$Tg_{\text{mix (HME System)}} = \frac{(x_1 \Delta C_{P1} Tg_1 + x_2 \Delta C_{P2} Tg_2)}{(x_1 \Delta C_{P1} + x_2 \Delta C_{P2})} \quad \text{Eq. (4)}$$

here Tg_1 and Tg_2, are the glass transition temperatures of drug and polymers, respectively, X_1 and X_2, are weight fractions of each of the components, respectively, and $\Delta Cp1$ and $\Delta Cp2$ is the change in the heat capacity at Tg_1 and Tg_2 respectively [26].

The Simha-Boyer rule is expressed as;

$$Tg_{\text{mix (HME System)}} = \frac{(x_1 Tg_1 + x_2 K_{12} Tg_2)}{(x_1 + x_2 K_{12})}$$

The constant K_{12} can be estimated as follows;

$$K_{12} = \frac{\rho 1 Tg_1}{\rho 2 Tg_2}$$

where ρ is the density of each component.

Figure 3(b) compares the T_g of the selected SD formulations (**20% P407 SD formulations**) studied predicted by the Couchman–Karasz equation and Simha-Boyer rule with the T_g values of the samples determined experimentally by DSC analysis. **Mixing an amorphous drug that has a low T_g and a high T_g polymer in an ASD leads to the development of an SD system with a T_g that is in between the T_g of each of the pure components. As the T_g of amorphous INM and PVP VA64 is 42.285°C and 109.94°C respectively, the T_g of each of the samples decreased as a function of drug concentration as expected (Fig. 3(b)).** A single T_g was detected as a result of the formation of a solid solution that is polymers and drug present within a **two-phase system** due to HME as shown in **Figure 2(b) and Figure 3(a),** which according to the Couchman-Karasz equation when drug and polymer are miscible the T_g of the extruded formulation should be between the T_gs of each of the components.

While the INM was transformed to the amorphous form, any formulations containing P407 retained the characteristics of the crystalline portion of this polymer. The DSC analysis confirmed the predicated hansen miscibility of the drug-polymer mixtures by demonstrating the existence of molecularly dispersed INM within the polymeric matrix. The absence of sharp melting endotherms in the SD formulations suggest that INM is partially dissolved within the polymeric carriers.

3.3. ATR-FTIR Studies

ATR-FTIR spectroscopy is one of the most widely used methods to detect the intermolecular interactions in SDs, such as hydrogen bonds between API's and polymer excipients. **PVP VA64 acts a proton acceptor through the carbonyl of the amide group and the vinyl acetate group,**[28] **while INM can act as a proton donor through the –OH group of the carboxylic acid.**[4] Both γ-INM and αINM exist as dimers with carboxylic acid groups of one molecule directly interacting with one on another in a cyclic acid-acid dimer.[29] Stabilisation of INM in the amorphous phase involves disrupting these intermolecular dimers and involving the carboxylic acid of INM in hydrogen bonding. **Figure 4(a)** illustrates the ATR-FTIR spectra of γ-INM, αINM, pure polymers, physical mixture and SD formulations (SD21 and SD25).

Pure INM (γ-INM) is characterized by principal absorption peaks and showed two strong **non-hydrogen bonding** C=O bands at 1714.00 cm^{-1}(free C=O of carboxylic acid) and 1690.00 cm^{-1} (acid-acid dimer C=O Stretch) respectively, the O-H Stretch of the acid is broad however it is superimposed on the sharp C-H stretches, as the free carboxylic acid O-H Stretch may exist as dimers via hydrogen bonding. In αINM this stretching shifts to 1707.00 cm^{-1} and 1679.00 cm^{-1} respectively.

Kolter, Karl and Gryczke.[28] reported that PVP VA64 due to its amide structure provide the drug molecule with hydrogen bond acceptors and thus acts as an appropriate polymeric carrier for the water-insoluble drug INM which result in thermodynamically stabilized dosage forms since their structure are similar to those of liquid based solutions. **These carbonyls which can act as proton accepters appear at 1731 cm^{-1} and 1672 cm^{-1} respectively as reported by Chan *et al.*[2] In this study this appeared to be the case as the main principal peaks appeared at 1731.00 cm^{-1} and 1670.00 cm^{-1} due to vinyl acetate and amide carbonyl respectively (Fig. 4(a)).** However, Chokshi *et al*.[27] also reported that there was no evidence of interaction between PVP VA64 and INM even though a shift was observed. In this study, there was evidence of chemical interaction between INM and PVP VA64.

The ATR-FTIR studies of all SD formulations with PVP VA64 and P407 may indicate that possible potential hydrogen bonding between the INM and PVPVA carbonyl is occurring, due to a broadening of the 1670 cm^{-1} PVP VA64 amide carbonyl peak to 1661 cm^{-1} as well as the appearance of a shoulder around 1650cm^{-1}.

Also, the intensity of the vinyl acetate C=O carbonyl did increase as the drug content increased, however, there was no shift in the vinyl acetate carbonyl peak **which possibly is because the amide carbonyl of PVP VA64 is a stronger proton acceptor compared to the vinyl acetate carbonyl of PVP VA64 as reported by Yuan *et al*.**[30]

It must be noted there was a greater broadening and a shift in the amide carbonyl as the % drug loading increased, this was also the case for SD formulations which contained no P407 as shown in Figure 4(b) and (c). This indicates that P407 possibly had no molecular interaction with INM and did not interfere in the interaction between INM and PVP VA64. In the case of the physical mixture, the amide C=O and vinyl acetate C=O stretch appeared at a much weaker intensity compared to the SD formulations, this may be because INM is still present in its crystalline form, therefore there was no interaction.

The shift and intensity of the carbonyl regions in the SD formulations are not very obvious even in the highest concentration of INM SD formulations. It was also found that this observation is a common phenomenon when FTIR is employed to detect intermolecular interactions in SDs because of the broad peak width and lower drug concentration. [31,32] Thus, it is necessary to have some solid evidence provided from different analytical techniques such as Raman spectroscopy or ssNMR spectroscopy to confirm the formation of hydrogen bonds between INM and PVP VA64.

3.4. SEM Studies

SEM was used to examine the surface morphology of the SD formulations and pure INM. The particle morphology of pure INM, pure polymers and SDs are illustrated in Figure 5. Pure P407 (Fig. 5(a)) appeared as smooth-surfaced spherical particles. Pure INM (Fig. 5(C)) appear irregular in size and shape and were much smaller than the P407 and SD particles. PVP VA64 appeared as spheres that are hollow in nature (Fig. 5(b)). While examining the physical mixture (Fig. 5(d)) no specific interaction was observed between drug and matrix material. From the SEM image of the SD (Fig. 5(e)), the INM crystals seem to be incorporated into the polymer matrix. From the SEM images, it can be deduced that the drug was successfully dispersed in the carrier material. No agglomeration was present resulting in a smooth surface and showed that the individual surface properties of PVP VA64, P407 and INM were lost during the extrusion process indicating INM possibly may be present in its amorphous form.

3.5. Phase Solubility Studies

The phase solubility plot of solubility of INM (µg/ml) against combined polymer concentration (% w/v) exhibits a linear relationship (which is *AL* type of plot) in the polymer concentration range that was investigated (Fig.6).

Table 3 shows that all Gibbs free energy of transfer values are negative at all carrier levels, this demonstrates that the drug solubilization process is spontaneous.[33] In drug-polymer SD mixtures the entropy of mixing is always favored and thus negative.

A-type phase solubility profiles are obtained when the solubility of the drug INM increases with increasing polymer concentration. When the complex is first order in nature with respect to ligand (polymeric matrix) and linear with respect to the substrate (drug), then the AL-type phase solubility profile is obtained.[34] The AL-type phase-solubility curve is obtained when the solubility curve is first order with respect to polymer concentration.[35]

Under AL-type phase-solubility diagram, the kinetic solubility of the API dispersed within a water - soluble polymer can be described with the slope (S) of the solubility curve and the intrinsic solubility (So) of the drug. As the concentration of carrier increased the ΔG^{0}_{tr} values decreased as the process at higher carrier levels is more favourable.

Table 3 also shows that INM-P407–PVP VA64 mixture has more favorable interactions in pH buffer 1.2 due to its higher *Ka* value compared to INM-P407 and INM-PVP VA64 mixtures respectively. In both cases, the solubility of INM increased as the polymeric carrier concentration increased. A negative value of *K*a signifies an increase in solubility. In this study, all *K*a values were positive indicating an increase in the kinetic solubility of INM at pH 1.2.

The *Ka* value represents the higher solubility gained from a metastable state of the compound. For example, amorphous drugs have a higher solubility than their crystalline counterparts but this solubility is unstable as the amorphous form has a tendency to revert to crystalline form. Thus it is referred to as the apparent stability constant, negative values signify a decrease in the solubility.

3.6. *In-Vitro* Dissolution Studies

The dissolution was performed under non-sink conditions in pH buffer 1.2 for 3 hours and pure INM was used as a control. **Non-sink conditions was used to determine the supersaturated drug concentration, which could be achieved by each SD formulation.** Pure crystalline INM is a weak acid with a pKa of 4.5 and displays pH-dependent solubility and dissolution rates; hence pH buffer 1.2 was used. **The AUC was calculated to examine any statistical difference (*p < 0.05) between the SD formulations, pure INM and amorphous INM.**

The phase solubility studies showed that the kinetic solubility of INM in aqueous solutions of P407 and PVP VA64 was 28 μg/ml (Fig.7). However, the kinetic solubility achieved during real - time dissolution was 21 μg/ml. This is because when the polymer and drug mixtures in the dry state were dispersed in aqueous polymer solutions, the polymer particles hydrated rapidly because of the high hydrophilic potency of P407 into polymer solution contributing to the increased wettability of the drug particles.[36] Enhanced solubility and dissolution of INM from physical mixtures could thus be related to the surface activity, wetting effect which may lead to reduced agglomeration and hence increased surface area, and solubilizing effect of P407.

The kinetic solubility of INM in all SD formulations increased in comparison to crystalline and amorphous INM respectively. Pure INM had a kinetic solubility of 1.2 μg/ml as expected, which is good agreement with the value reported in the literature.[37] **Pure amorphous INM has a kinetic solubility of 2.4 μg/ml as expected due to the conversion to the amorphous form**. The increase in kinetic solubility was dependent on polymer concentration.

There is a trend that as the P407 is increased so too does the concentration of drug in solution (Fig.7). The **kinetic solubility** of INM was increased by at least 10 times over 3 hours compared to the kinetic solubility of INM reported by Chokshi *et al*.[27]. Chokshi *et al*.[27] prepared binary mixtures of INM-PVP VA64 and **reported a kinetic solubility of 10 μg/ml for all SD formulations using 30%, 50% and 70% INM drug loading in pH buffer 1.2.**

There was also an improvement in solubility achieved from the 25% drug load formulations in comparison to the 20% drug load formulations. This is shown in Figure 7 where the maximum kinetic solubility achieved from the 20% INM SD formulations was 12 μg/ml. It can be concluded from the obtained results that 0.55:0.2:0.25 ratio (SD25) was found to be superior to other ratios of the polymer.

The AUC values of each of the SD formulations was compared to the crystalline INM and aINM using a one-way ANOVA and Tukey Kramer post-hoc test (Fig.7). For the 20% SDs and 25% SDs. **There was no statistical difference between crystalline INM and amorphous INM for all SD formulations except for SD19, SD20, SD24 and SD25. SD20 and SD25 which were statistically different to pure and amorphous INM and SD19 and SD24 were only statistically different to pure INM.** The overall effect of drug loading and % wt of polymer did have an effect on AUC and solubility of INM in solution.

The increase in the kinetic solubility of INM solid dispersions may be due to the reduction in the drug crystallinity and its colloidal and molecular dispersion within the polymeric carriers. As the polymeric carrier dissolved, the drug was exposed to dissolution medium in the form of very fine particles resulting in rapid dissolution.[38] P407 existed in solution as a unimer but self-assembled into micelles. At concentrations that are above the critical micelle concentration, unimer molecules aggregate to form micelles.[39] The hydrophobic P407 propylene oxide core of the micelle incorporated into the water-insoluble molecules of INM, which may have resulted in increased solubility of the drug molecule.[40]

It must be noted that apart from the higher hydrophilicity and surface properties of P407, increased wettability and dispersibility and particle size reduction of the drug,[40], also may have contributed to the improved kinetic solubility of INM. Higher hydrophilicity and surfactant properties of P407 result in greater wetting and increase the surface available by reducing interfacial tension between the water-insoluble drug and dissolution medium.

Park *et al*.[41] reported that high P407 loading can retard drug release, this may be due to the gelling property of poloxamer at higher concentrations, in this study this may also have been the case as recrystallization of the INM was shown at higher drug ratios of P407 and may have resulted in retarded drug release after 3 hours. As P407 was present in its semi-crystalline form, this may also have contributed to the recrystallization of the INM during *in-vitro* dissolution studies.

3.7. Accelerated stability studies

The 25 completely amorphous hot-melt extruded formulations were subjected to conditions of 40°C and 75% relative humidity for 5 months, after which hyper DSC was used to examine the crystalline content. Hyper DSC traces for the PVP VA64, P407 and INM formulations are illustrated in **Figure 8 (a) and (b)** and DSC traces of all the SD formulations are summarized in **Figure 8(a). Potter *et al*.[42] and Sinclair *et al*.[43] reported the relative instability of SD formulations as a result of moisture uptake due to the hygroscopic nature of PVP. As water can act as a plasticizer, it has been reported in literature that water can lower the glass transition temperatures of SD Formulations and enhances the mobility of polymer and drug.**[44]

As a result because the T_g of the SD formulations occurred between 90-110°C, it was necessary that all moisture was removed prior to DSC analysis. All SD formulations were dried over phosphorous pentoxide for 24 hours prior to DSC analysis. This was because the moisture was coming off at the same temperature that the T_g occurred.

After 5 months accelerated stability, the melt extrudate of the drug with PVP VA64 and P407 showed no depression in glass transition temperature compared to the initial T_g as a result of moisture removal and a single *T*g was obtained for all formulations which is shown in Figure 8(b). The consistent solid-state properties after storage at accelerated conditions suggest that amorphous INM was stable in melt extrudate with PVP VA64 and P407. It was observed that all SD formulations showed were amorphous even at high P407 and drug loadings. This was because there was no melting endotherm present in all SD formulations between 120 and 175°C.

Many authors have reported in the literature that P407 used within a binary mixture with poorly water soluble drugs can rapidly dissolve away and leads to conversion from amorphous to crystalline states, as P407 does not seem to interact at a molecular level with the drug. Monzural *et al*.[45], Vasconcelos, Sarmento and Costa.[12] and Ven den Mooter.[13] have also reported that the addition of semi-crystalline polymers can result in recrystallization of the API over long periods of time.

P407, which is semi-crystalline in nature, did not seem to have any effect on the amorphous stability of INM after 5 months and no recrystallization was observed, the SD formulations which contained 0% P407 were also amorphous. Therefore the addition of P407 did not contribute to the amorphous stability of the SD formulations as shown in Figure 8(b).

4. Conclusion

The DSC, XRPD and SEM analysis confirmed INM was converted to its amorphous form via the HME process. The solubility and dissolution rate was also significantly improved due to high energy amorphous form. **The T_g decreased with increasing drug concentration as expected.**

A glass transition of -67°C was detected for P407 and had no effect on the amorphous stability of SD formulations and no recrystallization was observed. P407 retained its semi-crystalline state in all SD formulations, however careful analysis of the SD formulations indicates that the glass transition of P407 at -67°C was not present.

ATR-FTIR studies of the SD formulations confirmed potential hydrogen bonding between the amide carbonyl of PVP VA64 and –OH group of the carboxylic acid of INM, also the intensity of the vinyl acetate carbonyl did increase as the drug content increased. **There was a greater broadening and a shift in the amide carbonyl as the % drug loading increased as a result of potential hydrogen bonding; this was also the case for SD formulations which contained no P407. This indicates that P407 possibly had no molecular or chemical interaction with INM and did not interfere in the interaction between INM and PVP VA64.**

Phase solubility studies of INM in aqueous solutions of P407 and PVP VA64 showed an increase in the kinetic solubility of INM compared with the pure drug at 37°C with a *K*a value of 0.041 µg/ml. **In the *In-vitro* dissolution studies it was observed that the kinetic solubility of INM was increased in SD formulations in comparison to crystalline and amorphous INM**. There was a trend that as the % P407 concentration increased so too did the concentration of drug in solution, with a kinetic solubility of 21 µg/ml.

However, it was observed that ternary mixtures prepared with the addition of P407 significantly improved drug release in comparison to many binary mixtures reported in literature prepared with INM and PVP VA64.

The **kinetic solubility** of INM was increased by at least 10 times over 3 hours compared to the kinetic solubility of INM reported by Chokshi *et al*.[27] with a maximum kinetic solubility of 21 µg/ml. **Chokshi *et al*.[27] prepared binary mixtures of INM-PVP VA64 using 30, 50 and 70% drug load and the kinetic solubility reported for the ASD formulations was 10 µg/ml respectively in pH 1.2. Also there was no depression in T_g as a result of moisture uptake compared to the binary mixtures of INM and PVP VA64 reported by Chokshi et al.[27] after 5 month's stability at 40°C/75% RH and no recrystallization was observed.**

It was also concluded that apart from the higher hydrophilicity and surface properties of P407, increased wettability and dispersibility and particle size reduction of the drug also may have contributed to the improved kinetic solubility of INM. P407 was also shown to retard drug release at high ratios of P407 due to the gelling properties of P407 at high concentrations. As P407 was present in its semi-crystalline form, this may have contributed to the recrystallization of the INM during *in-vitro* dissolution studies, therefore the ability to transform P407 from its semi-crystalline state to its amorphous state is a challenge that requires further research.

The stability data showed that the amorphous drug in solid solutions with PVP VA64 and P407 remained amorphous and no recrystallization was observed for all formulations and a single T_g was evident in all samples. Also it is important to note that P407 did not contribute to the amorphous stability of SD formulations.

In summary, T_g was not the only factor determining the stability of the amorphous formulations, but also the concentration of both drug and polymer played a significant role in the amorphous nature of INM. Thus a model drug with low T_g like INM can be stabilized by careful selection of both drug and polymer concentration. This study concluded that the amorphous solid dispersion contributed to the increased solubility of INM.

Note

The authors declare no competing financial interest.

Acknowledgments

This publication has emanated from research conducted with the financial support of the Synthesis and Solid State Pharmaceutical Centre, funded by Science Foundation Ireland under Grant 12/RC/2275.

References

1. Loftsson T, Brewster ME. Pharmaceutical applications of cyclodextrins: Basic science and product development. *J Pharm Pharmacol*. 2010;62(11):1607-1621.

2. Chan SY, Chung YY, Cheah XZ, Tan EYL, Quah J. The characterization and dissolution performances of spray dried solid dispersion of ketoprofen in hydrophilic carriers. *Asian J Pharm Sci*. 2015;10(5):372-385.

3. Lust A, Strachan CJ, Veski P, Aaltonen J, Heinämäki J, Yliruusi J, Kogermann K. Amorphous solid dispersions of piroxicam and Soluplus®: Qualitative and quantitative analysis of piroxicam recrystallization during storage. *Int J Pharm*. 2015;486(1-2):306-314.

4. Potter C, Tian Y, Walker G, McCoy C, Hornsby P, Donnelly C, Jones DS, Andrews GP. Novel supercritical carbon dioxide impregnation technique for the production of amorphous solid drug dispersions: A comparison to hot melt extrusion. *Mol Pharm*. 2015.

5. Davis MT, Potter CB, Mohammadpour M, Albadarin AB, Walker GM. Design of spray dried ternary solid dispersions comprising itraconazole, soluplus and HPMCP: Effect of constituent compositions. *Int J Pharm*. 2017;519(1-2):365-372.

6. Alshahrani SM, Lu W, Park J-B, Morott JT, Alsulays BB, Majumdar S, Langley N, Kolter K, Gryczke A, Repka MA. Stability-enhanced hot-melt extruded amorphous solid dispersions via combinations of Soluplus® and HPMCAS-HF. *AAPS PharmSciTech*. 2015;16(4):824-834.

7. Jondhale S, Bhise S, Pore Y. Physicochemical Investigations and Stability Studies of Amorphous Gliclazide. *Am Assoc Pharm Sci*. 2012;13(2):448-459.

8. Surwase SA, Itkonen L, Aaltonen J, Saville D, Rades T, Peltonen L, Strachan CJ. Polymer incorporation method affects the physical stability of amorphous indomethacin in aqueous suspension. *Eur J Pharm Biopharm*. 2015;96(June):32-43.

9. Baghel S, Cathcart H, O'Reilly NJ. Polymeric Amorphous Solid Dispersions: A Review of Amorphization, Crystallization, Stabilization, solid state characterization, and aqueous solubilization of biopharmaceutical classification system class II Drugs. *J Pharm Sci*. 2016;105(9):2527-2544.

10. Fousteris E, Tarantili PA, Karavas E, Bikiaris D. Poly(vinyl pyrrolidone)-poloxamer-188 solid dispersions prepared by hot melt extrusion: Thermal properties and release behavior. *J Therm Anal Calorim*. 2013;113(3):1037-1047.

11. Demuth B, Nagy ZK, Balogh A, Vigh T, Marosi G, Verreck G, Van Assche I, Brewster ME. Downstream processing of polymer-based amorphous solid dispersions to generate tablet formulations. *Int J Pharm*. 2015;486(1-2):268-286.

12. Vasconcelos T, Sarmento B, Costa P. Solid dispersions as strategy to improve oral bioavailability of poor water soluble drugs. *Drug Discov Today*. 2007;12(23-24):1068-1075.

13. Van Den Mooter G. The use of amorphous solid dispersions: A formulation strategy to overcome poor solubility and dissolution rate. *Drug Discov Today Technol*. 2012;9(2):e79-e85.

14. Chen Z, Liu Z, Qian F. Crystallization of bifonazole and acetaminophen within the matrix of semicrystalline, PEO-PPO-PEO triblock copolymers. *Mol Pharm*. 2015;12(2):590-599.

15. Zhu Q, Taylor LS, Harris MT. Evaluation of the microstructure of semicrystalline solid dispersions. *Mol Pharm*. 2010;7(4):1291-1300.

16. Gumaste SG, Gupta SS, Serajuddin ATM. Investigation of Polymer-Surfactant and Polymer-Drug-Surfactant Miscibility for Solid Dispersion. *AAPS J*. 2016;18(6).

17. Sun DD, Lee PI. Probing the mechanisms of drug release from amorphous solid dispersions in medium-soluble and medium-insoluble carriers. *J Control Release*. 2015;211:85-93.

18. Maniruzzaman M, Rana MM, Boateng JS, Mitchell JC, Douroumis D. Dissolution enhancement of poorly water-soluble APIs processed by hot-melt extrusion using hydrophilic polymers. *Drug Dev Ind Pharm*. 2012;39(2):218-227.

19. Greenhalgh DJ, Williams AC, Timmins P, York P. Solubility parameters as predictors of miscibility in solid dispersions. *J Pharm Sci*. 1999;88(11):1182-1190.

20. Yadav PS, Kumar V, Singh UP, Bhat HR, Mazumder B. Physicochemical characterization and in vitro dissolution studies of solid dispersions of ketoprofen with PVP K30 and d-mannitol. *Saudi Pharm J*. 2013;21(1):77-84.

21. Koda S, Shibata T, Park IS, Kojima S. Relaxation dynamics and fragility during liquid-glass transitions of poly(propylene glycol)s. *Curr Appl Phys*. 2015;15(7):805-810.

22. Assman K, Schneider HA. The thermal analysis of polymer blends of poly(ethylene oxide)/poly(hethyl hethacrylate). *J Therm Anal*. 1989;35:459-468.

23. Couchman PR, Karasz FE. A Classical Thermodynamic Discussion of the Effect of Composition on Glass-Transition Temperatures. *Macromolecules*. 1978;11(1):117-119.

24. Couchman PR. Compositional variation of glass transition temperatures. 2. Application of the thermodynamic theory to compatible polymer blends. *Macromolecules*. 1978;11:1156-1161.

25. Simha R, Boyer RF. On a General Relation Involving the Glass Temperature and Coefficients of Expansion of Polymers. *J Chem Phys*. 1962;37(5):1003-1007.

26. Pinal R. Entropy of mixing and the glass transition of amorphous mixtures. *Entropy*. 2008;10(3):207-223.

27. Chokshi RJ, Shah NH, Sandhu HK, Malick AW, Zia H. Stabilization of low glass transition temperature indomethacin formulations: Impact of polymer-type and its concentration. *J Pharm Sci*. 2008;97(6):2286-2298.

28. Kolter K, Karl M, Gryczke A. *Introduction to Solid Dispersions*.; 2012.

29. Taylor LS, Zografi G. Spectroscopic characterization of interactions between PVP and indomethacin in amorphous molecular dispersions. *Pharm Res*. 1997;14(12):1691-1698.

30. Yuan X, Xiang T-X, Anderson BD, Munson EJ. Hydrogen Bonding Interactions in Amorphous Indomethacin and Its Amorphous Solid Dispersions with Poly(vinylpyrrolidone) and Poly(vinylpyrrolidone-co-vinyl acetate) Studied Using 13 C Solid-State NMR. *Mol Pharm*. 2015;12:4518-4528.

31. Kestur S, Taylor S. Role of polymer chemistry in influencing crystal growth rates from amorphous felodipine. *CrystEngComm*. 2010;12(8):2390-2397.

32. Andrews GP, Abu-Diak O, Kusmanto F, Hornsby P, Hui Z, Jones DS. Physicochemical characterization and drug-release properties of celecoxib hot-melt extruded glass solutions. *J Pharm Pharmacol*. 2010;62(11):1580-1590.

33. Shekhar H, Kant V. Thermodynamic investigation on solid dispersions of nicotinamide – sulphamerazine drug system. *Sci World*. 2013;11(11):52-57.

34. Jambhekar SS, Breen P. Cyclodextrins in pharmaceutical formulations I: Structure and physicochemical properties, formation of complexes, and types of complex. *Drug Discov Today*. 2016;21(2):356-362.

35. LOFTSSON T, MÁSSON M, BREWSTER ME. Self- association of cyclodextrins and cyclodextrin complexes. *J Pharm Sci*. 2004;93(5):1091-1099.

36. Newa M, Bhandari KH, Oh DH, Kim YR, Sung JH, Kim JO, Woo JS, Choi HG, Yong CS. Enhanced dissolution of ibuprofen using solid dispersion with poloxamer 407. *Arch Pharm Res*. 2008;31(11):1497-1507.

37. Tres F, Treacher K, Booth J, Hughes LP, Wren SAC, Aylott JW, Burley JC. Indomethacin-Kollidon VA64 Extrudates: A Mechanistic Study of pH-Dependent Controlled Release. *Mol Pharm*. 2016.

38. Save T, Venkitachalam P. Studies on solid dispersions of nifedipine. *Drug Dev Ind …*. 1992;18(15):1663-1679.

39. Vyas V, Sancheti P, Karekar P, Shah M, Pore Y. Physicochemical characterization of solid dispersion systems of tadalafil with poloxamer 407. *Acta Pharm*. 2009;4:453-461.

40. Dumortier G, Grossiord JL, Agnely F, Chaumeil JC. A review of poloxamer 407 pharmaceutical and pharmacological characteristics. *Pharm Res*. 2006;23(12):2709-2728.

41. Park YJ, Yong CS, Kim HM, Rhee JD, Oh YK, Kim CK, Choi HG. Effect of sodium chloride on the release, absorption and safety of diclofenac sodium delivered by poloxamer gel. *Int J Pharm*. 2003;263(1-2):105-111.

42. Potter C, Tian Y, Walker G, McCoy C, Hornsby P, Donnelly C, Jones DS, Andrews GP. Novel supercritical carbon dioxide impregnation technique for the production of amorphous solid drug dispersions: A comparison to hot melt extrusion. *Mol Pharm*. 2015;12(5):1377-1390.

43. Sinclair W, Leane M, Clarke G, Dennis A, Tobyn M, Timmins P. Physical Stability and Recrystallization Kinetics of Amorphous Ibipinabant Drug Product by Fourier Transform Raman Spectroscopy. *J Pharm Sci*. 2011;100:4687-4699.

44. Huang Y, Dai W-G. Fundamental aspects of solid dispersion technology for poorly soluble drugs. *Acta Pharm Sin B*. 2014;4(1):18-25.

45. Monzurul A, Mahmud H, Kibria G, Rahman H, Ruknuzzaman R, Reza U. Dissolution enhnacement of poorly soluble carbamazepine by using polymeric solid dispersions. *Int J Pharm Sci Res*. 2010;2(1):49-57.

List of Tables

Table 1: Identifiers and compositions of the drug-polymer ratios studied in this work.

Identifier	INM [%wt]	P405 [%wt]
SD1	5	0
SD2	5	5
SD3	5	10
SD4	5	15
SD5	5	20
SD6	10	0
SD7	10	5
SD8	10	10
SD9	10	15
SD10	10	20
SD11	15	0
SD12	15	5
SD13	15	10
SD14	15	15
SD15	15	20
SD16	20	0
SD17	20	5
SD18	20	10
SD19	20	15
SD20	20	20
SD21	25	0
SD22	25	5
SD23	25	10
SD24	25	15
SD25	25	20

Table 2: Calculated Hansen Solubility Parameters for INM and each polymer.

Compound	δ_t ($MPa^{1/2}$)	$\Delta\delta$ ($MPa^{1/2}$)
INM	23.00	
PVP VA64	26.40	3.40
P407	25.50	2.50

Table 3: Gibbs free energy values and apparent stability constants (K_a) of INM-P407, INM-PVP VA64 and INM-P407-PVP VA64 interactions.

Concentration of P407 (%w/v)	Concentration of PVP VA64 (%w/v)	Quantity of INM added (mg)	Combined Concentration of Polymer (% w/v)	ΔG^0_{tr} (kJ/mol)		
				P407	PVP VA64	P407 + PVP VA64
0	45	**50**	45	0.00	-2.44	**-4.46**
5	55	**50**	60	-3.38	-2.93	**-5.50**
10	65	**50**	75	-3.80	-3.27	**-6.05**
15	75	**50**	90	-5.37	-3.43	**-6.22**
20	85	**50**	105	-6.17	-3.58	**-7.29**
25	**95**	**50**	**120**	**-7.81**	**-3.92**	**-7.74**
Intercept			0.99×10^0	1.43×10^0	4.68×10^0	
Slope			0.98×10^0	0.05×10^0	0.26×10^0	
K_a (µg/ml)			0.001	0.034×10^0	0.041	

List of Figures

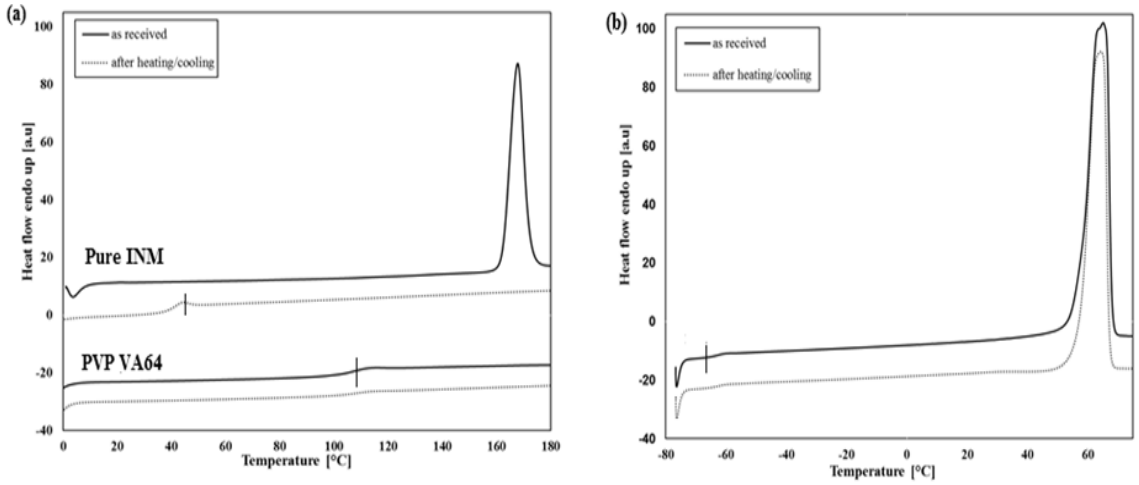

Figure 1: (a) DSC thermograms of pure INM and PVP VA64 as received and following heating at 100°C/min to 180°C. (b) DSC thermogram of pure P407 as received and following heating at 100°C/min. INM is transformed to the amorphous form but the semi-crystalline P407 retains its semi-crystalline morphology. *Tg* is indicated by a tick.

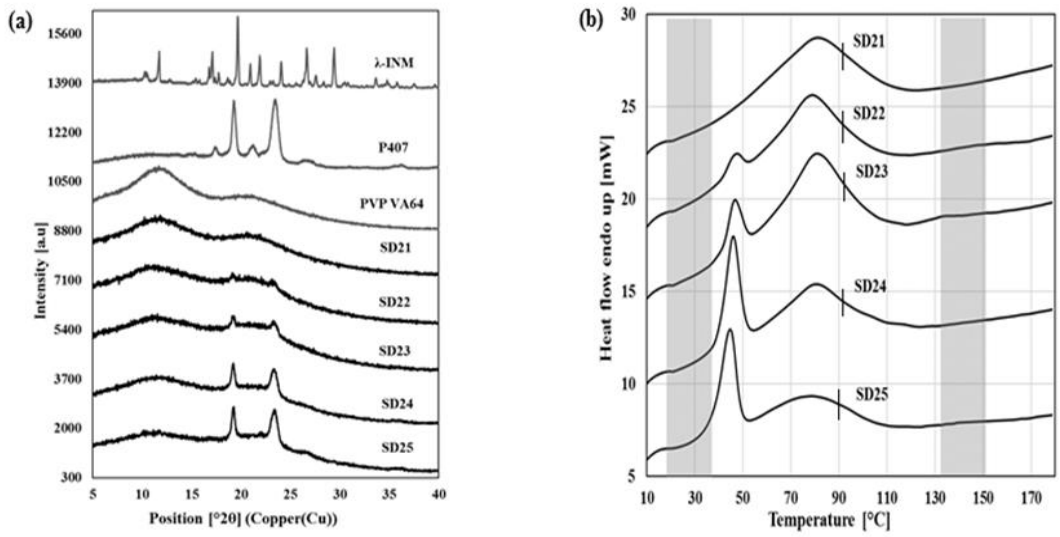

Figure 2: **(a) XRPD diffractograms and (b) DSC thermograms** of selected formulations indicating that the INM is present in the amorphous form but the P407 is not solubilised and exists in its crystalline form. **A single T_g is observed for all formulations, indicated by a tick.**

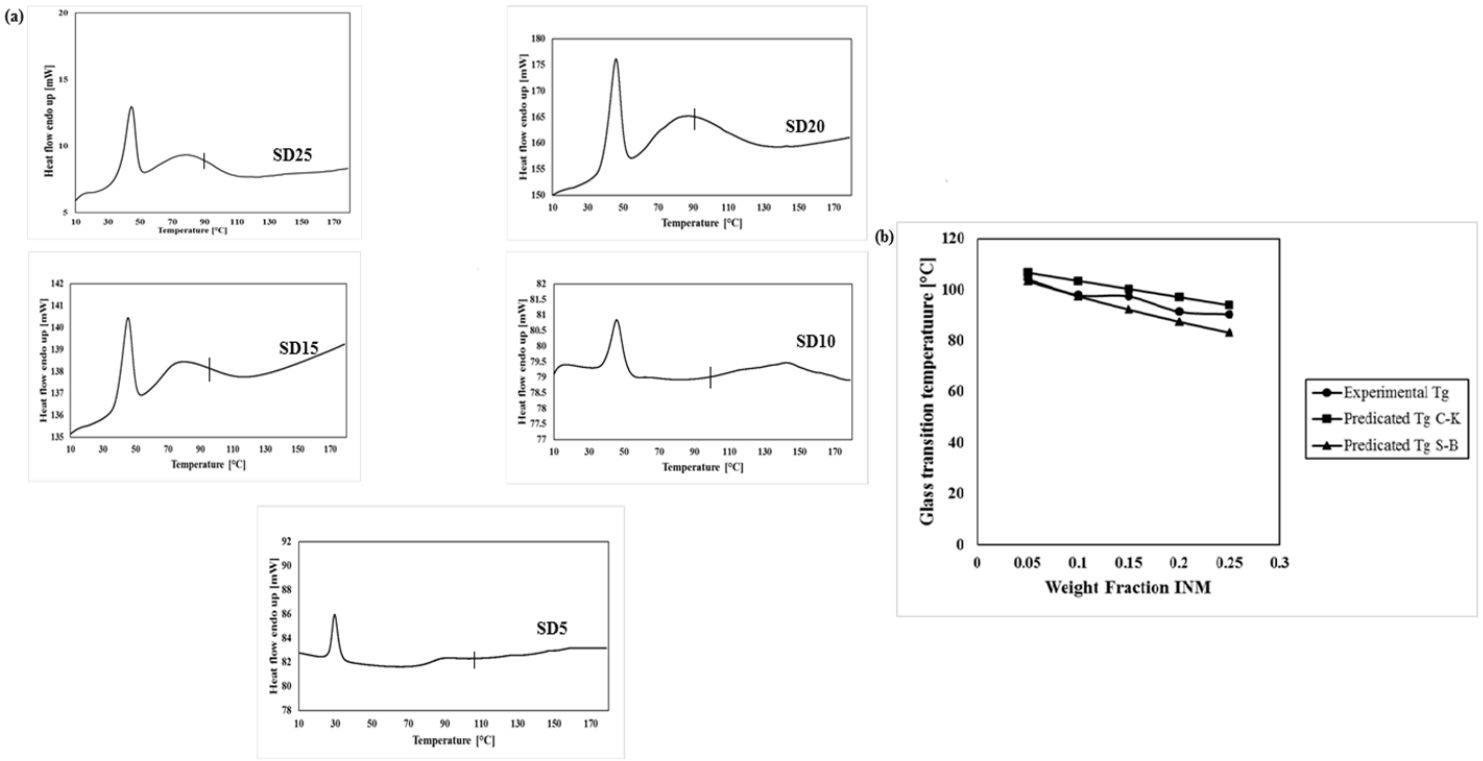

Figure 3(a): DSC thermograms of extruded SD formulations containing 20% P407 loading and Figure 3(b): Phase diagram of 20% P407 SD formulations extruded SD formulations indicating a dependence on both drug and P407 loading. Predicated T_g calculated using Couchman Karasz equation (C-K) and Simha-Boyer (S-B) rule. A single T_g is indicated by a tick.

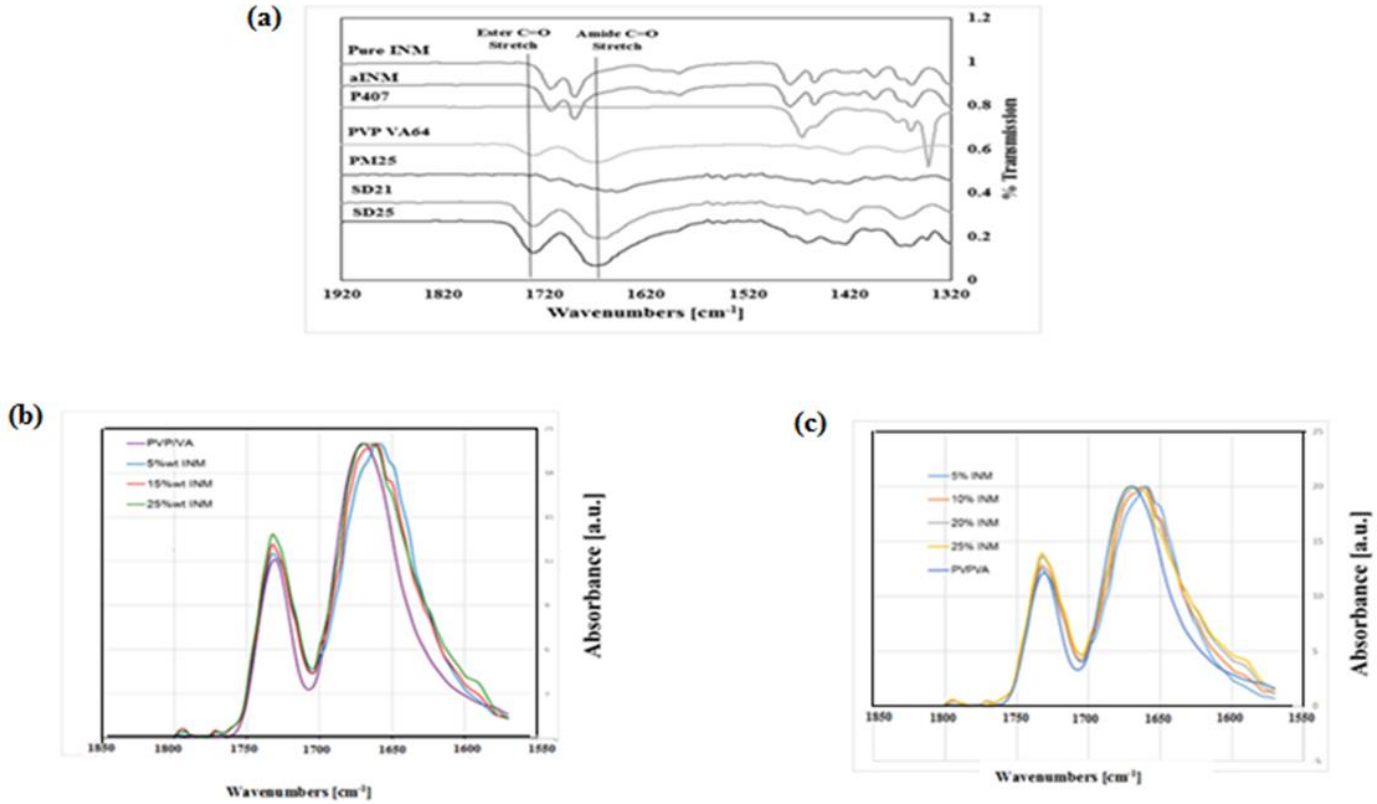

Figure 4 (a) : (Top) FTIR spectra of selected 25% SD formulations and pure components indicating a broadening of the amide carbonyl peak of PVP VA64 for both extruded dispersions. Figure 4 (b): (Bottom) SD formulations with 0% P407 loading and Figure 4 (c): (Bottom) SD formulations with 20% P407 loading.

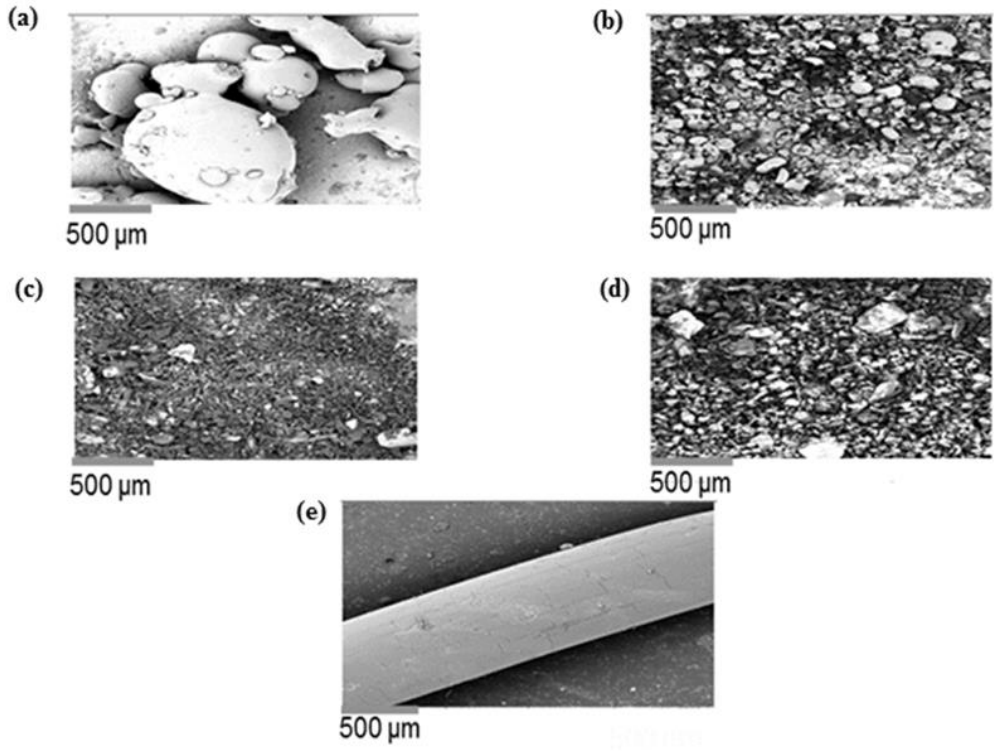

Figure 5: SEM images of Pure P407 (A), Pure PVP VA64 (B), Pure INM (C), PM (D) and ASD (E).

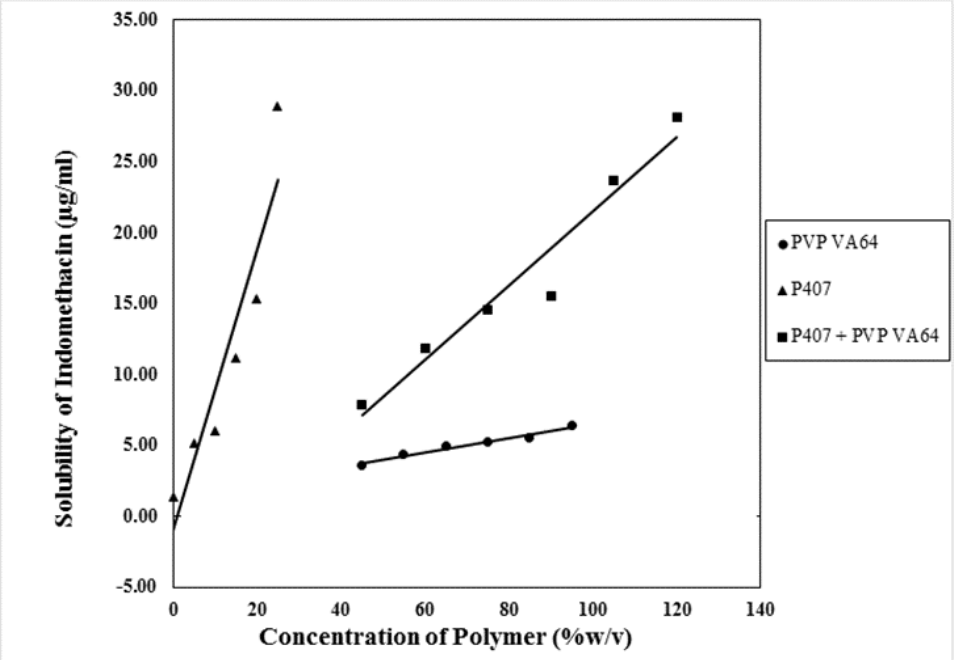

Figure 6: Solubility of INM (µg/ml) in aqueous solutions of PVP VA64 and P407 at 37°C (Each point represents the average ± SD of three independently prepared samples) with a maximum kinetic solubility of 28 µg/ml.

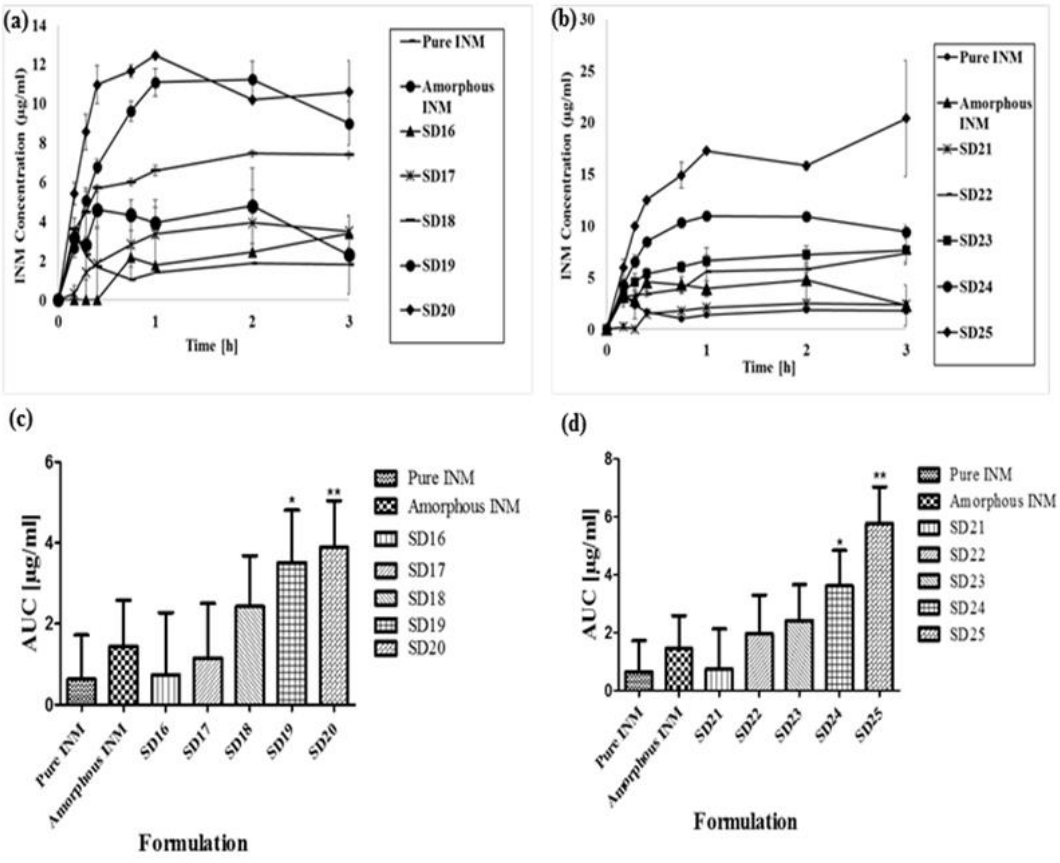

Figure 7: Dissolution profiles of (A) 20% INM SD formulations and (B) 25% INM SD formulations and Graphical representations of AUC for (C) 20% SD formulations and (D) 25% SD formulations in pH 1.2, **** and * represents statistical difference ($p < 0.05$) between ASD, pure INM and amorphous INM respectively, for a one way ANOVA and Tukey Kramer post-hoc test.**

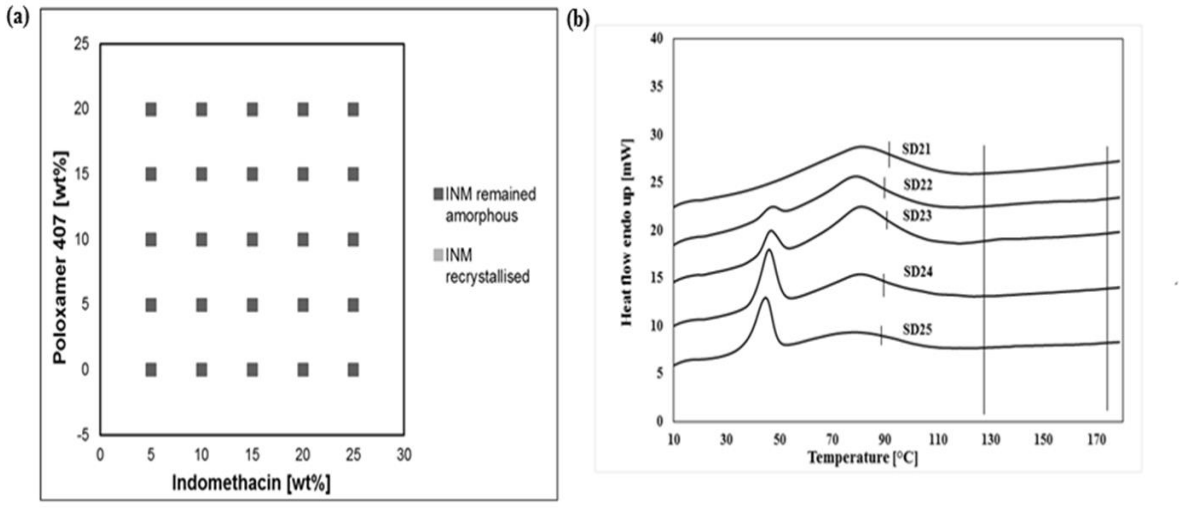

Figure 8(a): Hyper DSC traces of SD formulations after 5 months of a stability study under accelerated aging conditions of 40°C and 75% relative humidity. The heating rate utilized was 100°C/min. Figure 8 (b): Hyper DSC traces of 25% INM SD formulations. The area of interest of the γ-INM melting endotherm is marked by solid lines. A single T_g is indicated by a tick.